1521-009X/50/10/1389–1395$35.00
DRUG METABOLISM AND DISPOSITION

dx.doi.org/10.1124/dmd.121.000451
Drug Metab Dispos 50:1389–1395, October 2022

DRUG METABOLISM & DISPOSITION

Special Section on Mechanistic and Translational Research on Transporters in Toxicology

Attenuated Ochratoxin A Transporter Expression in a Mouse Model of Nonalcoholic Steatohepatitis Protects against Proximal Convoluted Tubule Toxicity

Joseph L. Jilek, Kayla L. Frost, Solène Marie, Cassandra M. Myers, Michael Goedken, Stephen H. Wright, and Nathan J. Cherrington

Department of Pharmacology and Toxicology, University of Arizona, College of Pharmacy, Tucson, Arizona (J.L.J., K.L.F., S.M., C.M.M., N.J.C.); Rutgers Translational Sciences, Rutgers University, Piscataway, New Jersey (M.G.); and Department of Physiology, University of Arizona, College of Medicine, Tucson, Arizona (S.H.W.)

Received March 9, 2021; accepted December 16, 2021

ABSTRACT

Ochratoxin A (OTA) is an abundant mycotoxin, yet the toxicological impact of its disposition is not well studied. OTA is an organic anion transporter (OAT) substrate primarily excreted in urine despite a long half-life and extensive protein binding. Altered renal transporter expression during disease, including nonalcoholic steatohepatitis (NASH), may influence response to OTA exposure, but the impact of NASH on OTA toxicokinetics, tissue distribution, and associated nephrotoxicity is unknown. By inducing NASH in fast food-dieted/thioacetamide-exposed mice, we evaluated the effect of NASH on a bolus OTA exposure (12.5 mg/kg by mouth) after 3 days. NASH mice presented with less gross toxicity (44% less body weight loss), and kidney and liver weights of NASH mice were 11% and 24% higher, respectively, than healthy mice. Organ and body weight changes coincided with reduced renal proximal tubule cells vacuolation, degeneration, and necrosis, though no OTA-induced hepatic lesions were found. OTA systemic exposure in NASH mice increased modestly from 5.65 ± 1.10 to 7.95 ± 0.61 mg*h/ml per kg BW, and renal excretion increased robustly from 5.55% ± 0.37% to 13.11% ± 3.10%, relative to healthy mice. Total urinary excretion of OTA increased from 24.41 ± 1.74 to 40.07 ± 9.19 μg in NASH mice, and kidney-bound OTA decreased by ~30%. Renal OAT isoform expression (OAT1–5) in NASH mice decreased by ~50% with reduced OTA uptake by proximal convoluted cells. These data suggest that NASH-induced OAT transporter reductions attenuate renal secretion and reabsorption of OTA, increasing OTA urinary excretion and reducing renal exposure, thereby reducing nephrotoxicity in NASH.

SIGNIFICANCE STATEMENT

These data suggest a disease-mediated transporter mechanism of altered tissue-specific toxicity after mycotoxin exposure, despite minimal systemic changes to ochratoxin A (OTA) concentrations. Further studies are warranted to evaluate the clinical relevance of this functional model and the potential effect of human nonalcoholic steatohepatitis on OTA and other organic anion substrate toxicity.

Introduction

Since the discovery of ochratoxin A (OTA) in 1965 (van der Merwe et al., 1965), the specific molecular mechanism of toxicity has yet to be determined (Malir et al., 2016). OTA is a well known mycotoxin that primarily contaminates foodstuffs, which serve as the primary route of exposure (Santos et al., 2009; Palumbo et al., 2015; Malir et al., 2016). Ochratoxins are naturally occurring metabolites produced by several fungi, including *Aspergillus* and *Penicillium* species, although OTA is considered the most toxic of the group (Bui-Klimke and Wu, 2015). Epidemiologic studies have linked OTA exposure to Balkan endemic nephropathy (Castegnaro et al., 2006; Yordanova et al., 2010), demonstrating that the kidney may be a target organ of toxicity. Indeed, given the prevalence of OTA in contaminated and spoiled foodstuffs, nephrotoxicity is a common finding in many animal species exposed to OTA, in addition to humans (Huff et al., 1975; Mally et al., 2005; Heussner and Bingle, 2015). Many mechanisms of toxic action have been proposed to explain OTA-induced renal damage (Simon et al., 1996), including apoptosis induction and reduced proximal tubule cell

This work was supported by National Institutes of Health National Institute of Environmental Health Sciences [Grant R01-ES028668], [Grant P30-ES006694], and [Grant T32-ES007091] (J.L.J.).

The authors declare they have no conflicts of interest with the contents of this article.

dx.doi.org/10.1124/dmd.121.000451.

ABBREVIATIONS: AUC, area under the plasma concentration-time curve; BCRP, breast cancer resistance protein; FFD/TH, fast food diet with thioacetamide; LC-MS/MS, liquid chromatography-tandem mass spectrometry; MRP, multidrug resistance-associated protein; NASH, nonalcoholic steatohepatitis; OAT, organic anion transporter; OATP, organic anion transporting polypeptide; OTA, ochratoxin A; P-gp, P-glycoprotein; $t_{1/2}$, elimination half-life; UPLC, Ultra Performance Liquid Chromatography.

adhesion, metabolism dysregulation, disruption of cellular electrochemical and pH homeostasis, and oxidative stress induction (Gekle and Silbernagl, 1993; Gekle et al., 1995; Schwerdt et al., 1999; Limonciel and Jennings, 2014). Though most evidence suggests that OTA selectively damages proximal convoluted tubule epithelial cells, glomerular changes may accompany chronic OTA exposure (Gekle and Silbernagl, 1994). Furthermore, OTA is an immunotoxicant (Al-Anati and Petzinger, 2006) and is also genotoxic in multiple species, including humans, necessitating the need for enhanced understanding of chronic exposure (Pfohl-Leszkowicz and Manderville, 2007; Stoev, 2010).

Toxicokinetic properties of xenobiotics are common variables in drug disposition and toxicity because slower drug clearance may exacerbate toxicity by increasing exposure. Furthermore, changes to systemic exposure may not always predict target organ toxicity, as transport-mediated uptake may concentrate certain toxicants into specific organs due to transporter isoform distribution and substrate specificity (Shitara et al., 2006; Hagos and Wolff, 2010). As a major xenobiotic clearance organ, the kidney expresses many specific transporters along the length of the nephron. Specifically, several organic anion transporter (OAT) isoforms are heavily expressed in proximal convoluted tubule cells of the renal cortex, where most xenobiotic active secretion and reabsorption from filtrate occurs (Masereeuw and Russel, 2001). Namely, OAT1 and 3 are expressed on the basolateral (blood) side, and although both are functionally bidirectional, they predominately import endogenous and exogenous solutes in coupled exchange for intracellular α-ketoglutarate (Nigam et al., 2015; Ivanyuk et al., 2017; Huo and Liu, 2018). OTA is negatively charged at physiologic pH and is a known substrate for OAT1 and 3 (Jung et al., 2001). Apical efflux of organic anions, including OTA, may be facilitated by transepithelial transport mediated by multidrug resistance-associated proteins (MRP) isoforms, including MRP2 and 4 and breast cancer resistance protein (BCRP), which efflux substrates into the renal filtrate (Anzai et al., 2010). Although these processes are unidirectional, apical OAT isoforms (OAT2 and 5 in rodents and OAT4 in humans) may also remove organic anion solutes from the filtrate, reabsorbing them back into the proximal tubule cell (Cha et al., 2000; Youngblood and Sweet, 2004; Anzai et al., 2005; Shima et al., 2010). Taken together, OTA renal elimination is a sum of OAT1/3-mediated secretion into the proximal convoluted tubule cell, efflux via MRP isoforms into the filtrate, passive filtration of the small amount unbound in plasma through the glomerulus, and any reabsorption from the filtrate via OAT2/5 in rodents (OAT4 in humans) (Anzai et al., 2010).

Interindividual variability in transporter expression is a known mediator of variable pharmacokinetics, tissue distribution, and toxicity (Meier et al., 2006; Prasad et al., 2014). These changes are often a result of genetic polymorphisms, sex, age, and disease (Urakami et al., 1999; Yonezawa et al., 2005; Nakanishi and Tamai, 2012; Mooij et al, 2014; Xu et al., 2017). Although many of these changes are inherited, disease progression may induce transporter expression changes that are not inherited (phenoconversion). Specifically, nonalcoholic steatohepatitis (NASH), the progressive and inflammatory stage of nonalcoholic fatty liver disease (NAFLD), has been shown to alter hepatic transporter expression in human and animal models of the disease, including specific organic anion transporting polypeptide (OATP) and MRP isoforms (Hardwick et al., 2011; Clarke et al., 2014; Clarke and Cherrington, 2015; Dzierlenga and Cherrington, 2018). Recently, our group has identified specific changes to renal transporters during NASH (Canet and Cherrington, 2014; Canet et al., 2015; Laho et al., 2016). Specifically, NASH-mediated changes to renal transporters have been shown to affect the disposition and toxicity of drugs, including renally cleared cisplatin (Jilek et al., 2021). However, renal disposition-related changes to the toxicity of organic anion substrates, such as OTA, have not yet been evaluated in an appropriate model.

To further understand changes to organic anion toxicokinetics and downstream effects on nephrotoxicity during NASH, we propose a fast food-dieted mouse with thioacetamide (FFD/TH) model to induce NASH. In this study, we demonstrate that reductions in renal OAT isoforms during NASH lead to increased urinary OTA clearance, and this in turn protects NASH mice from OTA-mediated nephrotoxicity.

Materials and Methods

Reagents. OTA and d5-OTA were purchased from Toronto Research Chemicals. Carboxymethyl cellulose, thioacetamide, and sodium deoxycholate were purchased from Sigma Aldrich. Liquid chromatography-mass spectrometry (LC-MS)-grade acetonitrile, water, ethyl acetate, and formic acid were purchased from Fisher Chemical. Sequencing-grade trypsin was purchased from Promega, Inc.

Animal Care and Use. All procedures were approved by the University of Arizona Institutional Animal Care and Use Committee and were carried out in accordance with the Guide for the Care and Use of Laboratory Animals. Five-week-old male C57BL/6J mice were purchased from Jackson Laboratories (Bar Harbor, ME) and acclimated for 1 week in polycarbonate cages (three mice per cage). After acclimation, mice were randomly split into healthy and NASH cohorts: eight mice were fed choline-sufficient and iron-supplemented L-amino acid rodent diet (Dyets Inc., Model No. 518754) to maintain healthy phenotype, and eight mice were fed an amino acid-defined fast food diet (Test Diets, Model No. AIN-76A) to induce the NASH phenotype, as previously demonstrated (Sharma et al., 2019). To induce hepatic inflammation consistent with a NASH phenotype, NASH mice were also administered thioacetamide (75 mg/kg i.p.) three times per week; thioacetamide was formulated at 10 mg/ml in sterile saline and then passed through a 0.2 μm filter. Water and test diets were available to mice ad libitum, and thioacetamide (for FFT/TH model mice only) was administered for 8 weeks to establish disease models.

OTA Exposure, Toxicokinetics, and Disposition. OTA was diluted to 1.25 mg/ml in 0.25% carboxymethyl cellulose in water and then filter sterilized by passing through a 0.2 μm filter. Four animals each from healthy and NASH cohorts were administered 12.5 mg/kg formulated OTA by oral gavage at t = 0 hours and then placed into metabolic cages; another four animals from each group were not exposed to OTA and were maintained as toxicant-naïve cohorts. After exposure, approximately 10 μl of whole blood was collected by submandibular venipuncture into heparinized tubes at t = 0.5, 1, 2, 3, 6, 12, 24, and 48 hours postdose and then centrifuged for 15 minutes at 4°C and 2000 × *g* to separate plasma. Urine was collected at 6, 24, 48, and 72 hours postdose by rinsing the metabolic cage with ∼5 ml of water to collect any urine that dried onto the metabolic cage funnel. At 8 hours postdose, mice were administered subcutaneous sterile saline (10 ml/kg) to account for repeated blood loss at early timepoints. At 72 hours postdose, animals were sacrificed by carbon dioxide overdose and terminal blood was collected into heparinized needles by cardiac puncture. Kidney and liver tissues were collected and snap-frozen in liquid nitrogen; a small slice of both tissues was preserved in 10% neutral buffered formalin prior to dehydration and embedding in paraffin for histopathology. All plasma, urine, and tissue samples were stored at −80°C until processed. Hematoxylin- and eosin-stained tissue sections were scored for the following by a board-certified veterinary pathologist: renal necrosis, degeneration, regeneration, proximal tubule vacuolation, tubule dilation, epithelial cell loss, and glomerular change; hepatic lipid accumulation, necrosis, apoptosis, inflammation, fibrosis, and biliary hyperplasia as previously described (Laho et al., 2016).

LC-MS/MS Measurement of OTA. Pure OTA stock standards were diluted to 10 mg/ml in dimethyl sulfoxide and used for all analytical procedures. To measure plasma and urine OTA concentrations, pure OTA was diluted directly into blank biologic matrices at the following concentrations to serve as analytical standards: 0.5, 1, 5, 12.5, 25, 50, and 100 μg/ml for plasma and 0.05, 0.125, 0.25, 0.5, 1, and 5 μg/ml for urine. Unknown plasma samples were quantified against calibrators by spiking 2 μl of either sample or calibrator into 50 μl water with 0.1% formic acid containing d5-OTA (internal standard) at a concentration of 400 ng/ml. Both analytes were extracted from the aqueous phase by liquid-liquid extraction with 1.25 ml ethyl acetate. One milliliter of the organic phase was dried over air and then reconstituted in 100 μl of 20:80

TABLE 1

OTA transporter surrogate peptides and multiple reaction monitoring method used for this study
Membrane protein fractions were digested with trypsin to quantify transporter expression.

Protein	Peptide Sequence	IS	RT *min*	Q1 $[M + 2H]^{2+}$ *Da*	Q3 $[M + H]^{+}$ *Da*
P-gp	IATEAIENFR	BCRP-H	15.8	582.3	979.5
BCRP	ENLQFSAALR	BCRP-H	16.5	574.8	792.4
MRP2	GINLSGGQK	MRP2-H	9.8	437.2	703.4
MRP3	QGELQLLR	MRP2-H	10.0	366.2	501.3
MRP4	APVLFFDR	MRP4-H	19.9	482.8	697.4
OAT1	TSLAVLGK	OAT1-H	14.0	394.7	600.4
OAT2	VGGFGPFQLR	MRP4-H	20.4	539.3	864.5
OAT3	DITSAK	MRP2-H	4.8	317.7	406.2
OAT5	ILSQDDLLR	BCRP-H	16.1	536.8	846.4
OATP4C1	DFPTAVK	OAT1-H	12.2	389.2	515.3
MRP2-H	GINL*SGGQK	—	9.8	440.7	710.4
MRP4-H	TSLA*VLGK	—	20.4	486.3	704.4
BCRP-H	ENLQFSA*ALR	—	16.5	576.9	668.4
OAT1-H	TSLA*VLGK	—	14.0	396.7	491.3

Multiple reaction monitoring transitions used for detection are listed as doubly charged parent ion (Q1) and singly charged fragment ion (Q3) used for quantification.
* Indicates $^{13}C/^{16}N$ heavy isotope labeled amino acid internal standards (IS). RT indicates retention time for liquid chromatography method. — Indicates that no IS was used.

acetonitrile:water with 0.1% formic acid prior to LC-MS/MS analysis. Unknown urine samples were quantified against calibrators by spiking 20 µl of either sample or calibrator into 200 µl water with 0.1% formic acid containing d5-OTA at a concentration of 50 ng/ml. Both analytes were extracted from the aqueous phase by liquid-liquid extraction with 1 ml ethyl acetate. Eight hundred microliters of organic phase were dried over air and then reconstituted in 100 µl of 20:80 acetonitrile:water with 0.1% formic acid prior to LC-MS/MS analysis.

To measure tissue-bound OTA, a small slice of tissue was weighed and added to ice-cold 80:20 methanol:water with 200 ng/ml d5-OTA at a ratio of 0.5 ml per 25 mg tissue and homogenized using a rotary tissue grinder. Two hundred microliters were aliquoted and centrifuged for 10 minutes at 20,000 and 4°C to remove debris; then 100 µl of supernatant was diluted with 1 ml water with 0.1% formic acid. Analytes were purified by liquid-liquid extraction with 1 ml ethyl acetate, vortexed, and then centrifuged for 2 minutes at 300 × *g* to separate phases. A 500 µl aliquot was dried over air and then reconstituted with 200 µl 20:80 acetonitrile:water with 0.1% formic acid prior to LC-MS/MS analysis. To quantify OTA in unknown tissue samples, blank tissue (kidney or liver) was homogenized in the same d5-OTA-spiked buffer at a ratio of 0.5 ml per 25 mg tissue. The homogenate was then spiked with pure OTA and serially diluted to generate 31.25, 62.5, 125, 250, and 500 ng/ml calibrators and then processed in the same manner as unknown samples. Quantified unknown samples were converted to OTA mass per 25 mg tissue based on the volume-to-tissue ratio.

Extracted samples were separated and quantified by LC-MS/MS using an Agilent Ultra Performance Liquid Chromatography (UPLC) system connected to a Sciex QTrap 6500+ triple quadrupole tandem mass spectrometer. Two microliters of each sample were injected onto a Luna Omega Polar C18 1.6 µm bead diameter UPLC column (Phenomenex) with 50 × 2.1 mm dimensions using an autosampler. Analyte separation was achieved by binary gradient where mobile phase A is water with 0.1% formic acid and mobile phase B is acetonitrile with 0.1% formic acid as follows: column equilibration at 20% B for 1 minute, 20% to 90% B over 4 minutes, 90% B for 1 minute, 90% to 20% B over 0.5 minutes, re-equilibration at 20% B for 1 minute. All analytes were ionized for mass spectrometric detection using positive electrospray ionization with the following source parameters: 5.5 kV electrospray voltage, 500°C source temperature, 20 psi curtain gas, 25 psi nebulizer gas, and 25 psi turbo gas. OTA and d5-OTA were detected using multiple reaction monitoring using 404.2 > 239.0 and 409.2 > 239.0 mass transitions, respectively, with the following parameters: 80 V declustering potential, 10 V entrance potential, 37 eV collision energy, 15 V collision cell exit potential. The LC-MS/MS system was operated using Analyst software, and analyte peak areas were integrated and quantified using MultiQuant software. All calibration curves were computed using linear regression with $1/x^2$ weighting with $R^2 \geq 0.99$; all unknown values for each biologic matrix or tissue fell within the limits of each respective calibration curve.

Surrogate Peptide Quantification of OTA Transporters. Kidney and liver tissue membrane fractions were prepared by ultracentrifugation and digested with trypsin; then unique surrogate peptides of OTA transporters were quantified by LC-MS/MS as previously described (Jilek et al., 2021). Briefly, tissue was homogenized on ice in 10 mM tris buffer with protease inhibitor (Pierce) and then centrifuged to remove debris at 8000 × *g* for 10 minutes. Supernatants were collected and membrane fractions were pelleted by ultracentrifugation at 100,000 × *g* for 1 hour at 4°C. The pellet was rinsed and then reconstituted with 10 mM tris buffer (pH 8.0); then 300 µg of protein was diluted into digestion buffer containing 3.7% (w/v) sodium deoxycholate 100 mM ammonium bicarbonate. Protein was reduced at 95°C for 5 minutes with 6 mM dithiothreitol and then alkylated at room temperature in the dark with 15 mM iodoacetamide; the alkylation reaction was quenched with 20 mM dithiothreitol, and then peptides were digested with trypsin/Lys-C (Pierce) at 37°C overnight using an enzyme:substrate ratio of 1:100. The next day, the digestion reaction was quenched with 0.4% formic acid containing heavy-labeled peptide standards (Table 1) and centrifuged for 30 minutes at 20,000 × *g* and 4°C to remove detergent. Peptides were extracted and concentrated from the supernatants by strong cation exchange solid phase extraction (1 mg MCX cartridges, Waters, Inc.) following the manufacturer instructions. Eluted peptides were dried using a vacuum centrifuge and then reconstituted in 50 µl starting LC-MS/MS mobile phase conditions, and 10 µl was injected onto an Acquity UPLC HSS C18 column (Waters, Inc.) using an Agilent autosampler and then separated by binary gradient flow using water and acetonitrile with 0.1% formic acid as previously described (Jilek et al., 2021). Surrogate tryptic peptides were then detected on a Sciex Qtrap 6500+ triple quadrupole tandem mass spectrometer using multiple reaction monitoring (Table 1). Peak areas were integrated and quantified against pure peptide

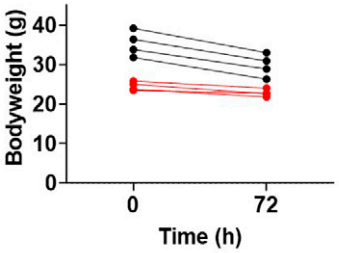

	ΔBW % of t=0	Kidney Mass mg/g BW	Liver Mass mg/g BW
• Healthy	-15.68 ± 1.20	11.01 ± 0.92	40.71 ± 2.51
• NASH	-7.00 ± 2.63*	12.53 ± 0.26*	53.23 ± 4.87*

Fig. 1. NASH animals administered 12.5 mg/kg OTA presented with less body weight and tissue loss after 72 hours compared with healthy mice. Individual body weights were measured at t = 0 and t = 72 hours study time, and change in body weight was determined relative to t = 0. Kidney and liver masses were measured at sacrifice and normalized to body weight. Mean values ± S.D. (n = 4 mice per group) were compared by unpaired two-tailed Student's t test where * indicates $P < 0.05$.

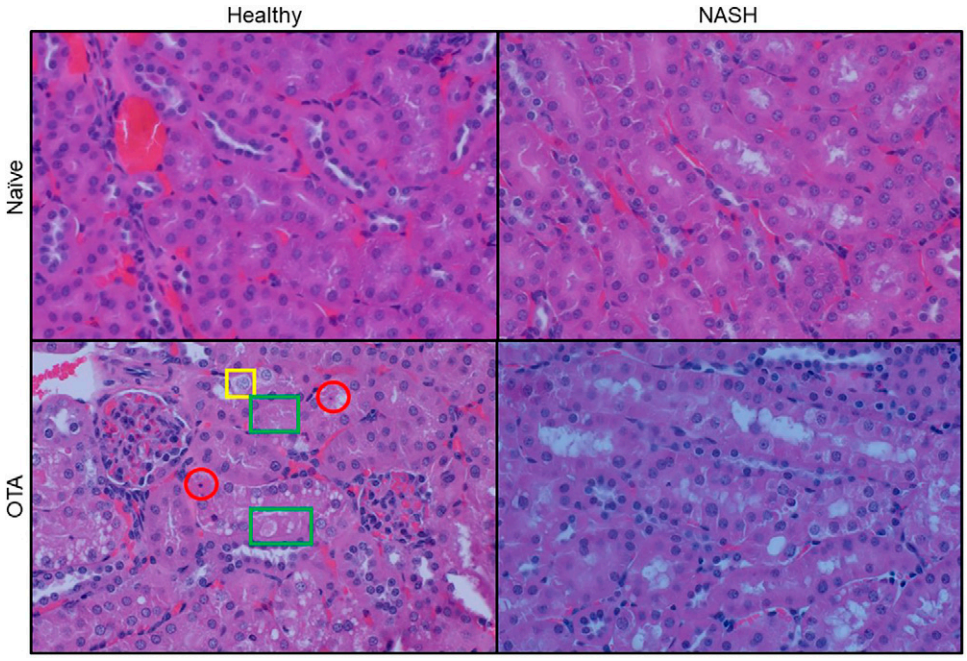

Fig. 2. Proximal tubule lesions are more prevalent in OTA-exposed healthy mice than in OTA-exposed NASH mice. Kidney slices were obtained from OTA-exposed and OTA-naïve mice in both healthy and NASH cohorts. Necrotic (red circles), degenerative (yellow boxes), and cell loss lesions (green boxes) were more frequently observed in the proximal convoluted tubules of healthy OTA-exposed mice than in NASH OTA-exposed mice. Formalin-fixed and paraffin-embedded kidney slides were stained with hematoxylin and eosin; representative images were captured at 200× magnification.

standards (Table 1) and protein abundance was converted to picomole per milligram (pmol/mg) protein using the following equation:

$$Protein\ Abundance\ \left(\frac{pmol}{mg\ Protein}\right) = \frac{Surrogate\ Peptide\ (pg)}{Peptide\ MW\ \left(\frac{g}{mol}\right)} \times \frac{1}{Peptide\ Input\ (mg)} \quad (1)$$

Pharmacokinetics Modeling and Data Analysis. Plasma OTA pharmacokinetic parameters were derived by the area under the plasma concentration-time curve (AUC) method using Phoenix WinNonlin version 8.1 (Certara, Inc.). Renal excretion as a percentage of dose was calculated by the percentage of total amount of OTA eliminated into the urine over 72 hours to the bolus dose by oral gavage. Grouped analysis represents mean values ± S.D. Means were compared using two-tailed Student's *t* test or analysis of variance (ANOVA) where appropriate (GraphPad Prism 9.0); comparisons were considered significantly different when $P < 0.05$.

Histopathology. Kidney samples were fixed in 10% neutral-buffered formalin prior to routine processing and paraffin embedding. Tissue sections (5 μm) were stained with hematoxylin and eosin and examined/analyzed by a board-certified veterinary pathologist. Renal sections were examined for necrosis, degeneration, vacuolation, regeneration, tubular dilation, epithelial cell loss, and glomerular changes. Semiquantitative severity scores were as follows: 0, none; 1, minimal with less than 10% affected; 2, mild with 10%–25% affected; 3, moderate with 25%–40% affected; 4, marked with 40%–50% affected; and 5, severe with over 50% affected.

Results

NASH Mice Display Reduced OTA-Associated Nephrotoxicity. After a single 12.5 mg/kg bolus dose of OTA (by mouth), healthy and NASH mice lost 7.00% ± 2.63% and 15.68% ± 1.20% of baseline body weight, respectively, suggesting that OTA may be generally less toxic in NASH mice (Fig. 1). At sacrifice, both kidney and liver masses of control mice decreased by approximately 12% and 30% more than those of NASH mice treated with the same dose of OTA per kg of body weight (Fig. 1). These findings were supported by histopathological lesions in the kidney but not in the liver of OTA-exposed treatment groups. Specifically, necrosis scores increased significantly from minimal (score of 1) in

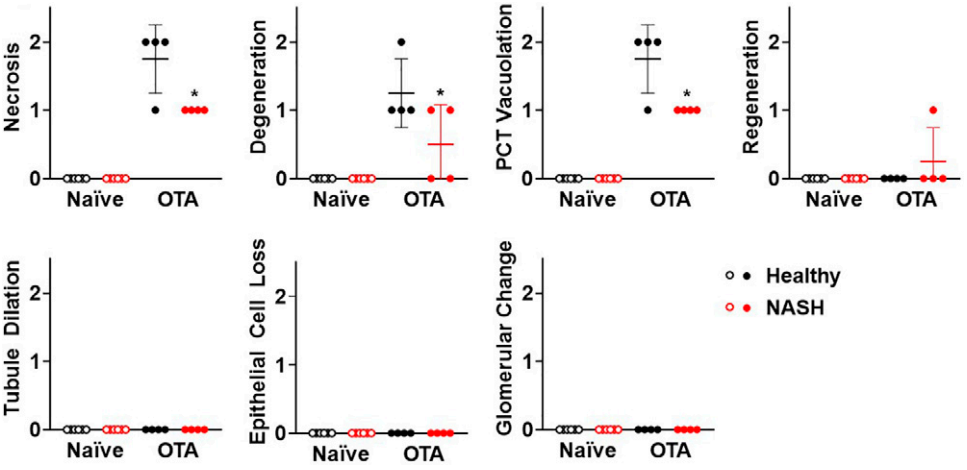

Fig. 3. Necrotic and degenerative lesions and proximal convoluted tubule cell vacuolation are more prevalent in healthy OTA-exposed mice than in NASH OTA-exposed mice. Significant increases in necrosis, degeneration, and proximal convoluted tubule (PCT) vacuolation were observed in healthy OTA-exposed animals, relative to NASH OTA-exposed animals. No histomorphological findings were observed in the kidney of OTA-naïve mice. Points represent individual animals, and horizontal bars represent mean values ± S.D. Mean values were compared by one-way ANOVA with Sidak's post hoc test where * indicates $P < 0.05$.

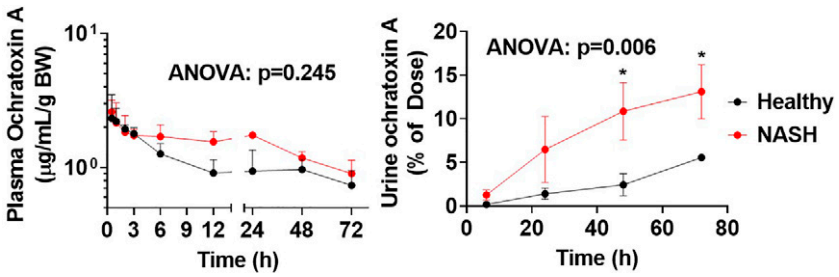

Fig. 4. NASH increases urinary OTA excretion but does not significantly alter plasma OTA concentrations. Plasma OTA concentrations over 72 hours were measured by LC-MS/MS and compared between NASH and healthy groups, and no significant changes were observed between both groups (right panel). OTA excreted into the urine was measured by LC-MS/MS throughout the study, and the mass of OTA recovered in the urine was calculated as a percentage of the bolus dose. Data points represent mean values ± S.D. of $n = 4$ animals per group and were compared by two-way ANOVA with Sidak's post hoc test where * indicates $P < 0.05$.

NASH mice to mild (score of 2) in healthy mice (Figs. 2 and 3). Similar significant histopathological trends were observed for the endpoint of proximal convoluted tubule cell vacuolation with reduced findings in the NASH/OTA group when compared with the healthy/OTA group (Fig. 3). Furthermore, degeneration of proximal convoluted tubule epithelial cells was decreased where half of the NASH mice presented with no degenerative lesions, whereas all healthy mice exhibited at least mild degenerative lesions in response to OTA (Fig. 3). There were no histopathological findings in OTA-naïve mice.

OTA Renal Excretion Increases in NASH Mice. To probe the differential nephrotoxicity induced by OTA in healthy and NASH mice, tissue distribution and OTA elimination were compared between both groups. Although individual mean plasma OTA concentrations over 72 hours did not vary significantly between groups, the plasma concentration-time curve trended upwards in the NASH mice, relative to healthy mice (Fig. 4). This was confirmed by a significant increase in dose-normalized plasma AUC_{last} from 5.65 ± 1.10 mg·h/ml per mg OTA in healthy animals to 7.95 ± 0.61 mg·h/ml per mg OTA (Table 2). However, the observed dose-normalized C_{max} in both groups was nearly identical at approximately 200 μg/ml per mg OTA, and the elimination half-life did not change significantly either. Notably, these changes were reflected in an approximately 33% decrease in apparent volume of distribution, suggesting that OTA may be accumulating in tissues at a greater rate in healthy animals (Table 2). As such, kidney- and liver-bound OTA increased significantly in healthy animals by approximately 30% in both tissues, relative to NASH animals (Fig. 5).

Although systemic rates of elimination did not vary between both groups, the cumulative percentage of OTA eliminated into the urine robustly increased in NASH animals, and this difference became significant at 48 hours postdose (Fig. 4). At sacrifice, the total amount of OTA eliminated into the urine in NASH mice was nearly 2-fold higher than in healthy mice (Table 2). This change was reflected in a significant increase in renal excretion from 5.55% ± 0.37% in healthy mice to 13.11% ± 3.10% in NASH mice (Table 2).

NASH Induces Changes to OTA Transporters. Given changes to renal excretion and disposition of OTA, renal and hepatic transporter expression was quantified to probe a possible molecular mechanism for this difference. Using a surrogate peptide LC-MS/MS method, known organic anion transporters were absolutely quantified from renal and hepatic membrane fractions (Fig. 6). Notably, all OAT isoforms in the kidney decreased to various degrees and OAT2 in the liver decreased modestly in the NASH mice. Basolateral renal OTA uptake transporters, OAT1 and OAT3, decreased in NASH mice from 0.37 ± 0.07 to 0.19 ± 0.09 pmol/mg protein and 1.02 ± 0.43 to 0.29 ± 0.13 pmol/mg protein, respectively. Expression of OAT2 also decreased in the kidney and liver of NASH mice from 2.20 ± 0.19 to 1.22 ± 0.46 pmol/mg protein and from 3.03 ± 0.41 to 2.39 ± 0.30 pmol/mg protein, respectively. Lastly, NASH mice displayed a robust decrease of the apically expressed renal OAT5 transporter from 1.12 ± 0.09 to 0.49 ± 0.19 pmol/mg protein, relative to healthy mice. Interestingly, P-glycoprotein (P-gp) increased significantly in renal tissue of NASH mice from an extremely low abundance to approximately 1.25 pmol/mg protein, suggesting that it may be induced in this tissue during NASH (Fig. 6). Furthermore, renal MRP2 decreased by approximately half in NASH mice, relative to healthy, although hepatic MRP2 increased modestly in NASH mice. Lastly, BCRP, MRP3, and MRP4, which facilitate active organic anion export, did not change between NASH and healthy animals.

Discussion

The current understanding of the mechanism of OTA renal elimination is proposed to be the sum of active OAT1- and OAT3-mediated secretion into the proximal tubule cells and glomerular filtration of unbound OTA, less any OAT2- and OAT5-mediated uptake from the filtrate back into the proximal convoluted tubule cell (Anzai et al., 2010). Given the dramatic decreases of all OAT transporters (Fig. 6), these data suggest that renal secretion and reabsorption are functionally limited in NASH mice, reducing the exposure of the proximal tubule cell to OTA. Additionally, glomerular filtration removes the small fraction of OTA that is unbound to plasma proteins, and our data suggest that the OAT2 and 5 decreases in NASH animals (Fig. 6) reduce the amount reabsorbed. As such, we observed an increase in the cumulative OTA eliminated into the urine (Fig. 4), reflected in a significant increase in OTA renal excretion (Table 2). These observations are further supported by evidence that less OTA is bound to renal tissue in NASH mice, relative to healthy mice (Fig. 5), and that this also manifests in significant decreases in nephrotoxic lesions in NASH mice (Figs. 1 and 2).

TABLE 2

Pharmacokinetic parameters in healthy and NASH rats administered 12.5 mg/kg OTA
Mean values ± S.D. were compared by unpaired two-tailed Student's *t* test where * indicates P < 0.05.

	$t_{1/2}$ *h*	C_{max}/D $\mu g \cdot ml^{-1} \cdot mg^{-1}$	AUC_{last}/D $mg \cdot h \cdot ml^{-1} \cdot mg^{-1}$	V_z/F *ml*	CL/F $ml \cdot h^{-1}$	A_e *μg*	A_e % of dose
Control	62.46 ± 17.04	199.80 ± 79.25	5.65 ± 1.10	8.28 ± 1.51	0.10 ± 0.03	24.41 ± 1.74	5.55 ± 0.37
NASH	53.17 ± 19.38	196.90 ± 52.51	7.95 ± 0.61*	5.44 ± 0.41*	0.08 ± 0.02	40.07 ± 9.19*	13.11 ± 3.10*

A_e, amount excreted into urine over 72 h; AUC_{last}, area under the plasma concentration-time curve measured from 0 to 72 h; CL/F, apparent systemic clearance; C_{max}, maximal plasma concentration; D, dose; $t_{1/2}$, elimination half-life; V_z/F, apparent volume of distribution.

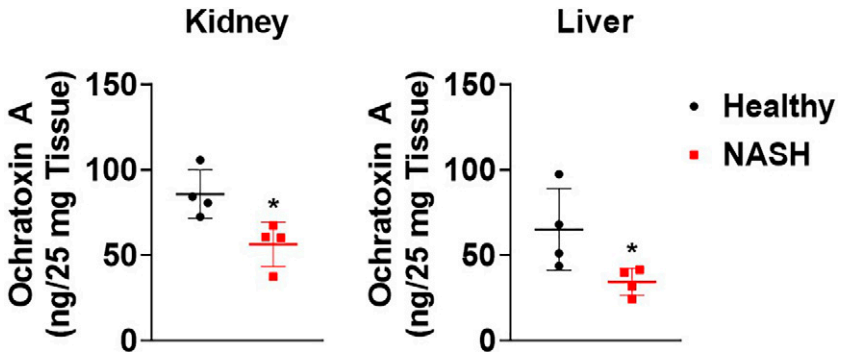

Fig. 5. NASH reduces kidney and liver disposition of a single OTA exposure. After 72 hours, the relative amount of OTA in kidney and liver tissue was measured by LC-MS/MS as described in *Materials and Methods*. Data points represent individual animal values, and horizontal bars represent mean values ± S.D. of $n = 4$ animals per group. Mean values were compared by unpaired two-tailed Student's t test where * indicates $P < 0.05$.

Taken together, these findings support a mechanistic protective effect of NASH-induced renal transporter phenoconversion.

OAT2 and 5 function is bidirectional (Anzai et al., 2005), consistent with other OAT isoforms, and in theory may function to secrete OTA into the filtrate via transepithelial transport after OAT1 and 3 uptake, in addition to reabsorption from the filtrate. As such, reduced OAT 2 and 5 expression in NASH mice (Fig. 6) exposed to OTA could either 1) sequester OTA that has been taken up by basolateral OATs in proximal convoluted tubule cells or 2) have a reduced capacity to reabsorb OTA from the tubular lumen. Although the data presented in this work do not prove the directionality of OAT2/5-mediated net OTA transport, these data suggest that OAT2/5 reductions induced by NASH reduce reabsorption into the proximal convoluted tubule cells.

NASH mice in this study demonstrated a significant decrease in basolateral OAT1/3 (Fig. 6), which may reduce proximal tubule cell disposition, as observed (Fig. 5). This may contribute to the observed reduction in nephrotoxicity in NASH mice (Fig. 3), as the plasma AUC also increased modestly (Table 2). However, average plasma concentrations at specific timepoints did not significantly differ between NASH and healthy animals (Fig. 4), nor did the rate of plasma OTA clearance (Table 2). Additionally, OTA is extensively plasma protein-bound, reducing the available pool of systemic OTA available for glomerular filtration and transport-mediated secretion (Ringot et al., 2006). Given the long elimination half-life in most species, including mice used in this study ($t_{1/2}$ ~50–60 hours, Table 2), it is unlikely that renal proximal tubule cells can accumulate a significant concentration gradient to shift the transport equilibrium to favor export of OTA. As such, these data, in addition to OTA physiochemical properties, suggest that reabsorption is a major driver of OTA nephrotoxicity.

Transport of OTA across biologic barriers is somewhat well understood; however, significant species differences exist. OAT5 is one of the primary apical OTA transporters, although it is not expressed in humans; likewise, OAT4 has significant substrate overlap with OAT5, including OTA, and is also expressed on the luminal membrane, but it is not expressed in rodents (Nigam et al., 2015; Ivanyuk et al., 2017). As such, although rodent OAT5 and human OAT4 share functional similarities, they are not true orthologs. Furthermore, although OAT2 expression is very low in the human kidney, our data suggest that absolute expression is appreciable in the mouse kidney (Fig. 2; Basit et al., 2019). Additionally, OAT2 expression in humans is localized to the basolateral membrane, whereas in rodents it is localized to the apical membrane (Ljubojevic et al., 2007; Nigam et al., 2015). Thus, while OAT4/5-dependent OTA reabsorption from the luminal filtrate is somewhat well studied, this species difference in rodents is not. Lastly, new OTA renal transporters are being identified, including human sodium/phosphate cotransporter 4 (hNPT4) (Jutabha et al., 2011); however, functional orthologs in rodents have not been identified to date.

Taken together, these results provide evidence suggesting that NASH-mediated decreases in several OAT isoforms reduce the kidney's capacity to accumulate OTA in an FFD/TH mouse model of NASH, thus reducing its nephrotoxicity. Additionally, as a major mechanism of organic anion clearance, NASH-induced disruptions to OAT

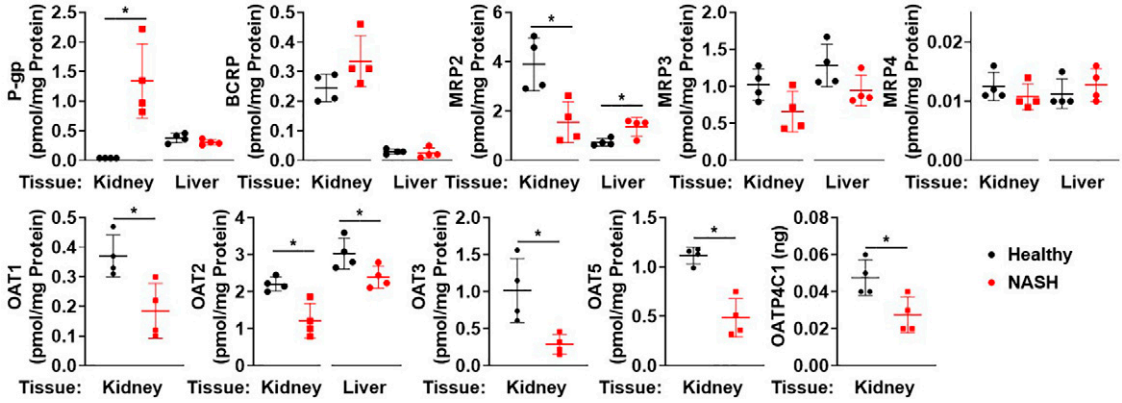

Fig. 6. OTA uptake transporter expression is altered in NASH mice. Transporter expression in liver and kidney tissue was evaluated by quantifying surrogate peptides. NASH animals showed significant decreases in basolateral OAT1 and 3 and apical OAT2 and 5 OTA uptake transporter expression. No significant changes were found in BCRP, MRP3, or MRP4 expression, which also catalyze OTA efflux, whereas renal P-gp and hepatic MRP2 expression increased. Data points represent individual animal values, and horizontal bars represent mean values ± S.D. of $n = 4$ animals per group. Mean values were compared by unpaired two-tailed Student's t test where * indicates $P < 0.05$.

expression likely affect renal elimination of other drugs and toxicants with similar physiochemical profiles. As such, this work highlights the importance of changes to reabsorption pathways, in addition to filtration and secretion during NASH, which may influence xenobiotic clearance, efficacy, or toxicity.

Authorship Contributions

Participated in research design: Jilek, Wright, Cherrington.

Conducted experiments: Jilek, Frost, Marie, Myers, Goedken.

Contributed new reagents or analytic tools: Jilek.

Performed data analysis: Jilek, Goedken.

Wrote or contributed to the writing of the manuscript: Jilek, Frost, Marie, Myers, Goedken, Wright, Cherrington.

References

Al-Anati L and Petzinger E (2006) Immunotoxic activity of ochratoxin A. *J Vet Pharmacol Ther* **29**:79–90.

Anzai N, Jutabha P, and Endou H (2010) Molecular mechanism of ochratoxin a transport in the kidney. *Toxins (Basel)* **2**:1381–1398.

Anzai N, Jutabha P, Enomoto A, Yokoyama H, Nonoguchi H, Hirata T, Shiraya K, He X, Cha SH, Takeda M, et al. (2005) Functional characterization of rat organic anion transporter 5 (Slc22a19) at the apical membrane of renal proximal tubules. *J Pharmacol Exp Ther* **315**:534–544.

Basit A, Radi Z, Vaidya VS, Karasu M, and Prasad B (2019) Kidney cortical transporter expression across species using quantitative proteomics. *Drug Metab Dispos* **47**:802–808.

Bui-Klimke TR and Wu F (2015) Ochratoxin A and human health risk: a review of the evidence. *Crit Rev Food Sci Nutr* **55**:1860–1869.

Canet MJ and Cherrington NJ (2014) Drug disposition alterations in liver disease: extrahepatic effects in cholestasis and nonalcoholic steatohepatitis. *Expert Opin Drug Metab Toxicol* **10**:1209–1219.

Canet MJ, Hardwick RN, Lake AD, Dzierlenga AL, Clarke JD, Goedken MJ, and Cherrington NJ (2015) Renal xenobiotic transporter expression is altered in multiple experimental models of nonalcoholic steatohepatitis. *Drug Metab Dispos* **43**:266–272.

Castegnaro M, Canadas D, Vrabcheva T, Petkova-Bocharova T, Chernozemsky IN, and Pfohl-Leszkowicz A (2006) Balkan endemic nephropathy: role of ochratoxins A through biomarkers. *Mol Nutr Food Res* **50**:519–529.

Cha SH, Sekine T, Kusuhara H, Yu E, Kim JY, Kim DK, Sugiyama Y, Kanai Y, and Endou H (2000) Molecular cloning and characterization of multispecific organic anion transporter 4 expressed in the placenta. *J Biol Chem* **275**:4507–4512.

Clarke JD and Cherrington NJ (2015) Nonalcoholic steatohepatitis in precision medicine: unraveling the factors that contribute to individual variability. *Pharmacol Ther* **151**:99–106.

Clarke JD, Hardwick RN, Lake AD, Lickteig AJ, Goedken MJ, Klaassen CD, and Cherrington NJ (2014) Synergistic interaction between genetics and disease on pravastatin disposition. *J Hepatol* **61**:139–147.

Dzierlenga AL and Cherrington NJ (2018) Misregulation of membrane trafficking processes in human nonalcoholic steatohepatitis. *J Biochem Mol Toxicol* **32**:e22035.

Gekle M, Pollock CA, and Silbernagl S (1995) Time- and concentration-dependent biphasic effect of ochratoxin A on growth of proximal tubular cells in primary culture. *J Pharmacol Exp Ther* **275**:397–404.

Gekle M and Silbernagl S (1993) Mechanism of ochratoxin A-induced reduction of glomerular filtration rate in rats. *J Pharmacol Exp Ther* **267**:316–321.

Gekle M and Silbernagl S (1994) The role of the proximal tubule in ochratoxin A nephrotoxicity in vivo: toxodynamic and toxokinetic aspects. *Ren Physiol Biochem* **17**:40–49.

Hagos Y and Wolff NA (2010) Assessment of the role of renal organic anion transporters in drug-induced nephrotoxicity. *Toxins (Basel)* **2**:2055–2082.

Hardwick RN, Fisher CD, Canet MJ, Scheffer GL, and Cherrington NJ (2011) Variations in ATP-binding cassette transporter regulation during the progression of human nonalcoholic fatty liver disease. *Drug Metab Dispos* **39**:2395–2402.

Heussner AH and Bingle LE (2015) Comparative ochratoxin toxicity: a review of the available data. *Toxins (Basel)* **7**:4253–4282.

Huff WE, Wyatt RD, and Hamilton PB (1975) Nephrotoxicity of dietary ochratoxin A in broiler chickens. *Appl Microbiol* **30**:48–51.

Huo X and Liu K (2018) Renal organic anion transporters in drug-drug interactions and diseases. *Eur J Pharm Sci* **112**:8–19.

Ivanyuk A, Livio F, Biollaz J, and Buclin T (2017) Renal drug transporters and drug interactions. *Clin Pharmacokinet* **56**:825–892.

Jilek JL, Frost KL, Jacobus KA, He W, Toth EL, Goedken M, and Cherrington NJ (2021) Altered cisplatin pharmacokinetics during nonalcoholic steatohepatitis contributes to reduced nephrotoxicity. *Acta Pharm Sin B* **11**:3869–3878.

Jung KY, Takeda M, Kim DK, Tojo A, Narikawa S, Yoo BS, Hosoyamada M, Cha SH, Sekine T, and Endou H (2001) Characterization of ochratoxin A transport by human organic anion transporters. *Life Sci* **69**:2123–2135.

Jutabha P, Anzai N, Hayashi K, Domae M, Uchida K, Endou H, and Sakurai H (2011) A novel human organic anion transporter NPT4 mediates the transport of ochratoxin A. *J Pharmacol Sci* **116**:392–396.

Laho T, Clarke JD, Dzierlenga AL, Li H, Klein DM, Goedken M, Micuda S, and Cherrington NJ (2016) Effect of nonalcoholic steatohepatitis on renal filtration and secretion of adefovir. *Biochem Pharmacol* **115**:144–151.

Limonciel A and Jennings P (2014) A review of the evidence that ochratoxin A is an Nrf2 inhibitor: implications for nephrotoxicity and renal carcinogenicity. *Toxins (Basel)* **6**:371–379.

Ljubojević M, Balen D, Breljak D, Kusan M, Anzai N, Bahn A, Burckhardt G, and Sabolić I (2007) Renal expression of organic anion transporter OAT2 in rats and mice is regulated by sex hormones. *Am J Physiol Renal Physiol* **292**:F361–F372.

Malir F, Ostry V, Pfohl-Leszkowicz A, Malir J, and Toman J (2016) Ochratoxin A: 50 years of research. *Toxins (Basel)* **8**:191.

Mally A, Völkel W, Amberg A, Kurz M, Wanek P, Eder E, Hard G, and Dekant W (2005) Functional, biochemical, and pathological effects of repeated oral administration of ochratoxin A to rats. *Chem Res Toxicol* **18**:1242–1252.

Masereeuw R and Russel FG (2001) Mechanisms and clinical implications of renal drug excretion. *Drug Metab Rev* **33**:299–351.

Meier Y, Pauli-Magnus C, Zanger UM, Klein K, Schaeffeler E, Nussler AK, Nussler N, Eichelbaum M, Meier PJ, and Stieger B (2006) Interindividual variability of canalicular ATP-binding-cassette (ABC)-transporter expression in human liver. *Hepatology* **44**:62–74.

Mooij MG, Schwarz UI, de Koning BA, Leeder JS, Gaedigk R, Samsom JN, Spaans E, van Goudoever JB, Tibboel D, Kim RB, et al. (2014) Ontogeny of human hepatic and intestinal transporter gene expression during childhood: age matters. *Drug Metab Dispos* **42**:1268–1274.

Nakanishi T and Tamai I (2012) Genetic polymorphisms of OATP transporters and their impact on intestinal absorption and hepatic disposition of drugs. *Drug Metab Pharmacokinet* **27**:106–121.

Nigam SK, Bush KT, Martovetsky G, Ahn SY, Liu HC, Richard E, Bhatnagar V, and Wu W (2015) The organic anion transporter (OAT) family: a systems biology perspective. *Physiol Rev* **95**:83–123.

Palumbo JD, O'Keeffe TL, Ho YS, and Santillan CJ (2015) Occurrence of ochratoxin a contamination and detection of ochratoxigenic Aspergillus species in retail samples of dried fruits and nuts. *J Food Prot* **78**:836–842.

Pfohl-Leszkowicz A and Manderville RA (2007) Ochratoxin A: an overview on toxicity and carcinogenicity in animals and humans. *Mol Nutr Food Res* **51**:61–99.

Prasad B, Evers R, Gupta A, Hop CE, Salphati L, Shukla S, Ambudkar SV, and Unadkat JD (2014) Interindividual variability in hepatic organic anion-transporting polypeptides and P-glycoprotein (ABCB1) protein expression: quantification by liquid chromatography tandem mass spectroscopy and influence of genotype, age, and sex. *Drug Metab Dispos* **42**:78–88.

Ringot D, Chango A, Schneider YJ, and Larondelle Y (2006) Toxicokinetics and toxicodynamics of ochratoxin A, an update. *Chem Biol Interact* **159**:18–46.

Santos L, Marín S, Sanchis V, and Ramos AJ (2009) Screening of mycotoxin multicontamination in medicinal and aromatic herbs sampled in Spain. *J Sci Food Agric* **89**:1802–1807.

Schwerdt G, Freudinger R, Mildenberger S, Silbernagl S, and Gekle M (1999) The nephrotoxin ochratoxin A induces apoptosis in cultured human proximal tubule cells. *Cell Biol Toxicol* **15**:405–415.

Sharma L, Gupta D, and Abdullah ST (2019) Thioacetamide potentiates high cholesterol and high fat diet induced steato-hepatitic changes in livers of C57BL/6J mice: a novel eight weeks model of fibrosing NASH. *Toxicol Lett* **304**:21–29.

Shima JE, Komori T, Taylor TR, Stryke D, Kawamoto M, Johns SJ, Carlson EJ, Ferrin TE, and Giacomini KM (2010) Genetic variants of human organic anion transporter 4 demonstrate altered transport of endogenous substrates. *Am J Physiol Renal Physiol* **299**:F767–F775.

Shitara Y, Horie T, and Sugiyama Y (2006) Transporters as a determinant of drug clearance and tissue distribution. *Eur J Pharm Sci* **27**:425–446.

Simon P, Godin M, and Fillastre JP (1996) Ochratoxin a: a new environmental factor which is toxic for the kidney? *Nephrol Dial Transplant* **11**:2389–2391.

Stoev SD (2010) Studies on carcinogenic and toxic effects of ochratoxin A in chicks. *Toxins (Basel)* **2**:649–664.

Urakami Y, Nakamura N, Takahashi K, Okuda M, Saito H, Hashimoto Y, and Inui K (1999) Gender differences in expression of organic cation transporter OCT2 in rat kidney. *FEBS Lett* **461**:339–342.

van der Merwe KJ, Steyn PS, Fourie L, Scott DB, and Theron JJ (1965) Ochratoxin A, a toxic metabolite produced by Aspergillus ochraceus Wilh. *Nature* **205**:1112–1113.

Xu YJ, Wang Y, Lu YF, Xu SF, Wu Q, and Liu J (2017) Age-associated differences in transporter gene expression in kidneys of male rats. *Mol Med Rep* **15**:474–482.

Yonezawa A, Masuda S, Nishihara K, Yano I, Katsura T, and Inui K (2005) Association between tubular toxicity of cisplatin and expression of organic cation transporter rOCT2 (Slc22a2) in the rat. *Biochem Pharmacol* **70**:1823–1831.

Yordanova P, Wilfried K, Tsolova S, and Dimitrov P (2010) Ochratoxin A and β2-microglobulin in BEN patients and controls. *Toxins (Basel)* **2**:780–792.

Youngblood GL and Sweet DH (2004) Identification and functional assessment of the novel murine organic anion transporter Oat5 (Slc22a19) expressed in kidney. *Am J Physiol Renal Physiol* **287**:F236–F244.

Address correspondence to: Dr. Nathan J. Cherrington, Department of Pharmacology and Toxicology, University of Arizona, College of Pharmacy, 1703 E. Mable Street, Tucson, AZ 85719. E-mail: cherrington@pharmacy.arizona.edu